Journal of Sound and Vibration (1998) **215**(3), 407–424
Article No. sv981647

OUT-OF-PLANE DYNAMIC RESPONSES OF NON-CIRCULAR CURVED BEAMS BY NUMERICAL LAPLACE TRANSFORM

C. S. HUANG

National Centre for Research on Earthquake Engineering, 200, *Sec*. 3, *Hsinhai Rd*., *Taipei*, *Taiwan*, *Republic of China*

AND

Y. P. TSENG AND S. H. CHANG

Department of Civil Engineering, *Tamkang University*, *Tamsui*, *Taiwan*, *Republic of China*

(*Received* 19 *November* 1997, *and in final form* 6 *March* 1998)

The paper presents a systematic method for analyzing the out-of-plane dynamic behaviours of non-circular curved beams the governing equations of which take into account the effects of shear deformation, rotary inertia, and viscous damping. The procedure consists of formulating an analytical solution for the transformed governing equations in the Laplace transform domain and computing the responses in the time domain by means of numerical Laplace inversion. As key elements in the dynamic stiffness method, the first known transformed dynamic stiffness matrix and equivalent nodal loading vector for non-circular curved beams subjected to distributed external loading are established from the analytical solution developed using the famous Frobenius method. With a simple modification, the formulation of the solution is also suitable for free vibration analysis, which results in an exact solution. As numerical examples for transient analysis, time responses of displacement components and stress resultants are found for a two-span elliptic beam subjected to a rectangular impulse. The behaviours of the responses due to the variation of the ratio of the long axis to the short one are investigated.

1. INTRODUCTION

As a very fundamental structural element in various structural systems, such as arch bridges, curved bridges, roof structures, piping systems, and aerospace structures, the dynamic behaviours of curved beams have been of interest to many researchers since the nineteenth century. Much of the research work is summarized in review articles [1–4], in which more than 600 articles have been reviewed. However, most of the literature has been devoted to various vibration problems of circular curved beams.

Much less research has focused on the out-of-plane vibrations of non-circular curved beams even though this type of curved beam is frequently found in practical situations. The Ritz method with different types of trial functions has often been applied in determining the natural frequencies of arches of various shapes [5, 6]. Chang and Volterra [7, 8] applied the Lehman–Maehly method to determine the upper and lower bounds of natural frequencies of curved beams. By combining the discrete Green function and a numerical integral technique, Kawakami *et al*. [9] developed an approximate solution for the in-plane and out-of-plane free vibrations of curved beams. With regard to analytical solutions, Suzuki and co-workers [10–12] developed a series solution in terms of

0022–460X/98/330407 + 18 $30.00/0

polynomials, in which the solutions for symmetric modes and anti-symmetric modes were considered separately while Irie *et al*. [13] and Huang *et al*. [14] used the transfer matrix method and the dynamic stiffness method, respectively.

Very few studies on the dynamic responses of a system consisting of non-circular curved beams have been reported in the literature. Irie *et al*. [15] used a transfer matrix approach to study the steady state responses of curved Timoshenko beams with internal hysteresis damping. Suzuki *et al*. [16] applied the modal superposition method to investigate the dynamic behaviours of a semi-elliptic arch subjected to a concentrated impulse without considering the effects of shear deformation and rotary inertia. It is well-known that many modes are needed to obtain accurate results for the responses of stress resultants and to accurately describe the concentrated impulse. Consequently, the modal superposition method may not be a good choice because of the complexity of determining natural frequencies and the corresponding mode shapes from the series solution developed by Suzuki *et al*. [10–12]. Apparently, investigation into the transient responses of plane curved beams has been insufficient.

In the present work, a methodology recently developed for analyzing the in-plane dynamic responses of arches [17] is extended to solve the out-of-plane ones. The procedure consists of formulating an exact solution for the transformed governing equations in the Laplace transform domain and computing the responses in the time domain using numerical Laplace inversion. Beskos and his co-workers [18–20] used a similar methodology to analyze the dynamic responses of a system consisting of straight members only. However, the out-of-plane dynamic responses of curved beams have not been analyzed using this procedure because two key elements have not yet been established, which are the dynamic stiffness matrix and the equivalent nodal loading vector for non-circular curved beams subjected to distributed external loading. Consequently, the main purpose of this paper is not only to present a systematic procedure for analyzing the out-of-plane dynamic behaviours of a system composed of non-circular curved beams, but also to formulate such dynamic stiffness matrix and equivalent nodal loading vector for a curved element. The latter is accomplished by using the well-known Frobenius method [21] to construct the analytical solution in the Laplace domain.

As numerical examples for transient analysis, the dynamic behaviours of two-span elliptic arches subjected to a rectangular impulse at the midpoint of the second span are investigated. The time responses of the displacement components (displacement, bending rotation angle, and twist angle) and the stress resultants (shear force, bending moment, and twisting moment) at the load point will be given to show the accuracy of the results. The behaviours of the responses due to the vibration of the ratio of the long axis to the short axis (a/b) will be discussed.

There are several important advantages to the proposed solution. It provides highly accurate dynamic responses not only for displacement components, but also for stress resultants, which are functions of the higher derivatives of the displacement, without any numerical difficulties. Because the analytical solution for a curved element is expressed in terms of a dynamic stiffness matrix, it is easy to combine this analytical solution with the dynamic stiffness matrices of other types of members to analyze the dynamic responses of a more complex system, such as an arch bridge or a space frame. The computer time needed for the present procedure to analyze a complex system can be much less than that needed by the conventional finite-element method with step-by-step time integration schemes, which was addressed by Beskos and Narayanan [20]. Compared with the traditional modal superposition method, the present method does not require knowledge of natural frequencies and modal shapes. Furthermore, when the dynamic responses of a system subjected to support motions are considered, a quasi-static solution [22] is required

in the modal superposition method, while the present method does not have this requirement.

2. GOVERNING EQUATIONS

A planar curved beam defined by its arc length S is shown in Figure 1, in which R represents the radius of the centroidal axis. Figure 1 also shows the stress resultants on the cross-section, namely, the bending moment (M_z), shear force (Q), and twisting moment (M_t), whose positive directions are given in the figure. The out-of-plane displacement of the centroidal axis is denoted by u while ζ and ϕ represent the bending rotation and the twist angle of the centroidal axis, respectively. By neglecting the warping deformation of the cross-section and considering the viscous damping effect, the well-known equations of motions for out-of-plane can be written as (cf. reference [4]):

$$\frac{\partial Q}{\partial S} = \rho A\ddot{u} + C_u\dot{u} - P_p, \tag{1a}$$

$$-\frac{\partial M_z}{\partial S} + \frac{M_t}{R} + Q = \rho I_z\ddot{\zeta} + C_\zeta\dot{\zeta}, \tag{1b}$$

$$\frac{\partial M_t}{\partial S} + \frac{M_z}{R} = \rho J\ddot{\phi} + C_\phi\dot{\phi}, \tag{1c}$$

where A and J, respectively, are the area and polar moment of the cross-section, ρ is the mass per unit volume, I_z is the second moment of the area of the cross-section about the Z-axis, and P_p is the distributed load. The viscous damping coefficients are set to be $C_u = \rho A\delta_u$, $C_\zeta = \rho I_z\delta_\zeta$, and $C_\phi = \rho J\delta_\phi$. The derivative with respect to time is denoted by a dot.

Based on the assumption of a linearly elastic material, the stress resultants are related to the displacement components by

$$Q = \kappa GA\left(\frac{\partial u}{\partial S} - \zeta\right), \tag{2a}$$

$$M_z = -EI_z\left(\frac{\partial \zeta}{\partial S} + \frac{\phi}{R}\right), \tag{2b}$$

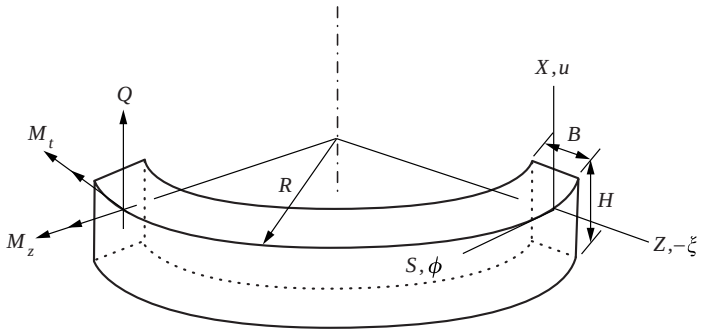

Figure 1. Curved beam co-ordinates and stress resultants for out-of-plane motion.

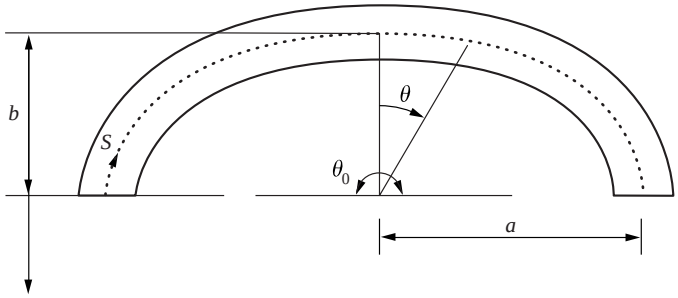

Figure 2. Configuration of an elliptic beam.

$$M_t = C\left(\frac{\partial \phi}{\partial S} - \frac{\zeta}{R}\right), \tag{2c}$$

where E and G are the Young's modulus and shear modulus, respectively, while κ and C are the shear coefficient and torsional stiffness coefficient of the cross-ection, respectively. The shear coefficient and torsional stiffness coefficient are dependent on the shape of the cross-section. The shear coefficient is used to take into account the variation of the shear deformation through the cross-section and is set equal to 0·85 for a rectangular cross-section and 0·89 for a circular cross-section for a beam with a Poisson's ratio of $v = 0{\cdot}3$ [23]. The torsional stiffness coefficient is used to take into account, to some extent, the effect of the warping deformation of the cross-section and is set equal to GJ for a circular cross-section while for rectangular cross-section (cf. reference [24]),

$$C = \frac{1}{3} GB^3 H\left(1 - \frac{192}{\pi^5}\frac{B}{H}\sum_{n=1,3,5}\frac{1}{n^5}\tanh\frac{n\pi H}{2B}\right), \tag{3}$$

where B and H are the width and the height of the cross-section, respectively. The summation in equation (3) converges very rapidly so that only the first term ($n = 1$) is used.

Substituting equations (2) into equations (1), assuming uniform cross-section and constant material properties through the curved beam, and performing transformation of co-ordinate S into θ shown in Figure 2 yields

$$\bar{u}'' + \bar{u}'\frac{\xi'}{\xi} - \frac{1}{\xi}\zeta' = \frac{\rho L^2}{E\lambda_1^2\xi^2}(\ddot{\bar{u}} + \delta_u\dot{\bar{u}}) - \frac{L}{EA\lambda_1^2\xi^2}P_p, \tag{4a}$$

$$\zeta'' + \frac{\xi'}{\xi}\zeta' - \left(\frac{\lambda_2^2}{\bar{r}^2\xi^2} + \frac{\lambda_1^2}{\bar{R}^2\xi^2}\right)\zeta + \left(\frac{1+\lambda_2^2}{\bar{R}\xi}\right)\phi' - \frac{\bar{R}'}{\bar{R}^2\xi}\phi + \frac{\lambda_1^2}{\bar{r}^2\xi}\bar{u}' = \frac{\rho L^2}{E\xi^2}(\ddot{\zeta} + \delta_\zeta\dot{\zeta}), \tag{4b}$$

$$\phi'' + \frac{\xi'}{\xi}\phi' - \frac{1}{\lambda_2^2\bar{R}^2\xi^2}\phi - \left(1 + \frac{1}{\lambda_2^2}\right)\zeta' + \frac{\bar{R}}{\bar{R}^2\xi}\zeta = \frac{\rho JL^2}{\xi^2 C}(\ddot{\phi} + \delta_\phi\dot{\phi}), \tag{4c}$$

where the primes denote the derivatives with respect to θ. In addition, the following non-dimensional quantities are introduced:

$$\bar{u} = u/L, \qquad \bar{R} = R/L, \qquad \xi = L(\mathrm{d}\theta/\mathrm{d}S), \qquad \lambda_1^2 = \kappa G/E, \qquad \lambda_2^2 = C/(EI_z),$$
$$\bar{\gamma}^2 = \gamma^2/L^2 = I_z/(L^2A), \tag{5}$$

where L is a representative length of the curved beam under consideration. Equations (4) are the governing equations for the out-of-plane motion of the non-circular curved beams. It should be noted that in some cases, such as when considering parabolic beams, the formulation of the solution will be simpler using Cartesian co-ordinates.

3. TRANSFORMED SERIES SOLUTION

To perform general dynamic analysis of a curved beam, the time domain is transformed into the Laplace domain. The main reason for using the Laplace transformation technique is not only that this technique was originally developed to solve initial value problems, but also that it is suitable for solving viscoelasticity problems due to the validity of the correspondence principle. Consequently, by assuming zero initial conditions, equations (4) become

$$\tilde{U}'' + \tilde{U}'\frac{\xi'}{\xi} - \frac{1}{\xi}\tilde{Z}' = \frac{\rho L^2}{E\lambda_1^2\xi^2}(s^2 + s\delta_u)\tilde{U} - \frac{L}{EA\lambda_1^2\xi^2}\tilde{P}_p, \tag{6a}$$

$$\tilde{Z}'' + \frac{\xi'}{\xi}\tilde{Z}' - \left(\frac{\lambda_2^2}{\bar{R}^2\xi^2} + \frac{\lambda_1^2}{\bar{r}^2\xi^2}\right)\tilde{Z} + \left(\frac{1+\lambda_2^2}{\bar{R}\xi}\right)\tilde{\Phi}' - \frac{\bar{R}'}{\bar{R}^2\xi}\tilde{\Phi} + \frac{\lambda_1^2}{\bar{r}^2\xi}\tilde{U}' = \frac{\rho L^2}{E\xi^2}(s^2 + s\delta_\zeta)\tilde{Z}, \tag{6b}$$

$$\tilde{\Phi}'' + \frac{\xi'}{\xi}\tilde{\Phi}' - \frac{1}{\lambda_2^2\bar{R}^2\xi^2}\tilde{\Phi} - \left(1 + \frac{1}{\lambda_2^2}\right)\frac{1}{\bar{R}\xi}\tilde{Z}' + \frac{\bar{R}'}{\bar{R}^2\xi}\tilde{Z} = \frac{\rho JL^2}{\xi^2 C}(s^2 + s\delta_\phi)\tilde{\Phi}, \tag{6c}$$

where $(\tilde{U}, \tilde{Z}, \tilde{\Phi}, \tilde{P}_p) = \int_0^\infty (\bar{u}, \zeta, \phi, P_p)\, \mathrm{e}^{-st}\, \mathrm{d}t$ and s is a complex number. Equations (6) are a set of second order ordinary differential equations for $\tilde{U}$, $\tilde{Z}$ and $\tilde{\Phi}$ with variable coefficients depending on θ only, which can be solved exactly using the well-known Frobenius method [21].

For convenience, the Taylor's expansion series of the variable coefficients and the external load function in equations (6) about a convenient position, say η, can be expressed as

$$\frac{\xi'}{\xi} = \sum_{k=0}^{K} a_k(\eta - \eta)^k, \qquad \frac{1}{\xi} = \sum_{k=0}^{K} b_k(\theta - \eta)^k, \qquad \frac{\bar{R}'}{\bar{R}^2\xi} = \sum_{k=0}^{K} d_k(\theta - \eta)^k,$$

$$\frac{1}{\bar{R}\xi} = \sum_{k=0}^{K} e_k(\theta - \eta)^k, \qquad \frac{1}{\bar{R}^2\xi^2} = \sum_{k=0}^{K} f_k(\theta - \eta)^k, \qquad \frac{\tilde{P}_p}{\xi^2} = \sum_{k=0}^{K} p_k(\theta - \eta)^k. \tag{7}$$

Hence, for the given geometry of a curved beam and external loading function, the coefficients a_k, b_k, c_k, d_k, e_k, f_k and p_k can be determined with the aid of commercial symbolic logic computer software packages like "Mathematica" or "MACSYMA". Using the Frobenius method, the solution to equations (6) are expressed in terms of polynomials as

$$\tilde{U} = \sum_{j=0}^{J} A_j(\theta - \eta)^j, \qquad \tilde{Z} = \sum_{j=0}^{J} B_j(\theta - \eta)^j \quad \text{and} \quad \tilde{\Phi} = \sum_{j=0}^{J} D_j(\theta - \eta)^j, \tag{8}$$

where coefficients A_j, B_j and D_j are functions of the Laplace transform parameter s. Theoretically, J in equation (8) should approach infinity if an exact solution is to be

obtained. Nevertheless, to obtain very accurate numerical results, only a sufficiently large number of terms in equation (8) is needed.

By substituting equations (7) and (8) into equations (6) and carefully collecting the terms which have the same order of polynomials, one can obtain the following recursive formulas for the relationships among the coefficients in equation (8):

$$A_{j+2} = \frac{-1}{(j+1)(j+2)} \left\{ \sum_{k=0}^{j} \left[(k+1)a_{j-k}A_{k+1} - (k+1)b_{j-k}B_{k+1} \right.\right.$$

$$\left.\left. - \frac{\rho L^2}{E\lambda_1^2}(s^2 + \delta_u s)c_{j-k}A_k \right] + \frac{L}{EA\lambda_1^2} p_j \right\}, \tag{9a}$$

$$B_{j+2} = \frac{-1}{(j+1)(j+2)} \sum_{k=0}^{j} \left[\frac{\lambda_1^2}{\bar{\gamma}^2}(k+1)c_{j-k}A_{k+1} + (k+1)a_{j-k}B_{k+1} \right.$$

$$\left. + (k+1)(1+\lambda_2^2)\, e_{j-k}\, D_{k+1} - \left(\left(\frac{\rho L^2(s^2 + \delta_\zeta s)}{E} + \frac{\lambda_1^2}{\bar{\gamma}^2} \right) c_{j-k} + \lambda_2^2 f_{j-k} \right) B_k - d_{j-k} D_k \right], \tag{9b}$$

$$D_{j+2} = -\frac{1}{(j+1)(j+2)} \sum_{k=0}^{j} \left[-(k+1)\left(1 + \frac{1}{\lambda_2^2}\right) e_{j-k}\, B_{k+1} + (k+1)a_{j-k}D_{k+1} \right.$$

$$\left. + d_{j-k}B_k - \left(\frac{\rho J L^2}{C}(s^2 + \delta_\phi s)c_{j-k} + \frac{f_{j-k}}{\lambda_2^2} \right) D_k \right], \tag{9c}$$

where $j = 0, 1, 2, \ldots$. From equations (9), coefficients A_{j+2}, B_{j+2}, and D_{j+2} for $j \geqslant 0$ can be determined if A_0, A_1, B_0, B_1, D_0 and D_1 are known. Consequently, the solution to equations (6) can be reduced to the following simple expression:

$$\tilde{U}(\theta) = A_0\tilde{u}_0(\theta) + A_1\tilde{u}_1(\theta) + B_0\tilde{u}_2(\theta) + B_1\tilde{u}_3(\theta) + D_0\tilde{u}_4(\theta) + D_1\tilde{u}_5(\theta) + \tilde{u}_p(\theta), \tag{10a}$$

$$\tilde{Z}(\theta) = A_0\tilde{\zeta}_0(\theta) + A_1\tilde{\zeta}_1(\theta) + B_0\tilde{\zeta}_2(\theta) + B_1\tilde{\zeta}_3(\theta) + D_0\tilde{\zeta}_4(\theta) + D_1\tilde{\zeta}_5(\theta) + \tilde{\zeta}_p(\theta), \tag{10b}$$

$$\tilde{\Phi}(\theta) = A_0\tilde{\phi}_0(\theta) + A_1\tilde{\phi}_1(\theta) + B_0\tilde{\phi}_2(\theta) + B_1\tilde{\phi}_3(\theta) + D_0\tilde{\phi}_4(\theta) + D_1\tilde{\phi}_5(\theta) + \tilde{\phi}_p(\theta), \tag{10c}$$

where $\tilde{u}_j$, $\tilde{\zeta}_j$ and $\tilde{\phi}_j$ ($j = 0, 1, 2, \ldots, 5$) are a set of homogeneous solutions to equations (6), which are polynomial functions of θ with coefficients determined from equations (9). Polynomial functions $\tilde{u}_p$, $\tilde{\zeta}_p$ and $\tilde{\phi}_p$ are a set of particular solutions to equations (6).

4. TRANSFORMED DYNAMIC STIFFNESS MATRIX AND LOADING VECTOR

To analyze a single span curved beam, one may want to solve the beam by treating the whole curved beam as an element and determine coefficients A_0, A_1, B_0, B_1, D_0 and D_1 from the boundary conditions. Instead, however, we will introduce the concept of the dynamic

stiffness method and decompose a curved beam into several elements, an approach which has several advantages over treating the whole beam as one element. One advantage is that highly accurate solutions can always be obtained by increasing the number of elements or by increasing the values of K and J in equations (7) and (8), respectively. Consequently, the numerical difficulties caused by using very large numbers for K and J as reported by Suzuki and Takahashi [12] can be easily avoided. In addition, one can save time and trouble in finding the higher order terms in the Taylor's expansion series for the complex geometric terms and loading term given in equation (7). Furthermore, the convergence of the series solution given by equation (8) can be guaranteed by decomposing a curved beam into more elements as long as its convergence radius is not equal to zero.

When a curved beam is decomposed into a number of elements, directly from equations (10), the end displacements for each element (see Figure 3) in the Laplace domain can be expressed as

$$\begin{Bmatrix} \hat{U}_0 \\ \tilde{Z}_0 \\ \tilde{\Phi}_0 \\ \hat{U}_1 \\ \tilde{Z}_1 \\ \tilde{\Phi}_1 \end{Bmatrix}_n = [\beta]_n \begin{Bmatrix} A_0 \\ A_1 \\ B_0 \\ B_1 \\ D_0 \\ D_1 \end{Bmatrix}_n + \begin{Bmatrix} \hat{u}_p(\theta_n) \\ \tilde{\zeta}_p(\theta_n) \\ \tilde{\phi}_p(\theta_n) \\ \hat{u}_p(\theta_{n+1}) \\ \tilde{\zeta}_p(\theta_{n+1}) \\ \tilde{\phi}_p(\theta_{n+1}) \end{Bmatrix}_n, \tag{11a}$$

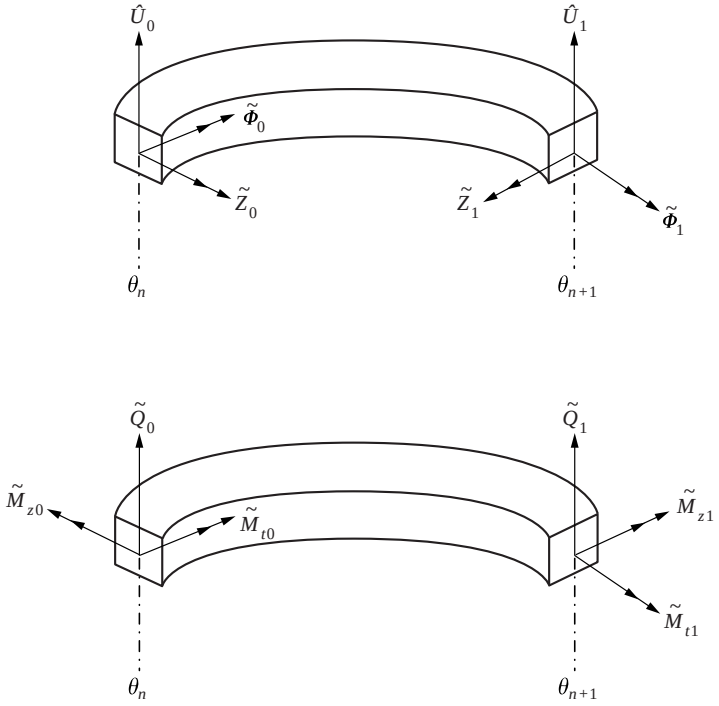

Figure 3. Positive displacement and stress resultants for the nth element.

where

$$[\beta]_n = \begin{bmatrix} \hat{u}_0(\theta_n) & \hat{u}_1(\theta_n) & \hat{u}_2(\theta_n) & \hat{u}_3(\theta_n) & \hat{u}_4(\theta_n) & \hat{u}_5(\theta_n) \\ \tilde{\zeta}_0(\theta_n) & \tilde{\zeta}_1(\theta_n) & \tilde{\zeta}_2(\theta_n) & \tilde{\zeta}_3(\theta_n) & \tilde{\zeta}_4(\theta_n) & \tilde{\zeta}_5(\theta_n) \\ \tilde{\phi}_0(\theta_n) & \tilde{\phi}_1(\theta_n) & \tilde{\phi}_2(\theta_n) & \tilde{\phi}_3(\theta_n) & \tilde{\phi}_4(\theta_n) & \tilde{\phi}_5(\theta_n) \\ \hat{u}_0(\theta_{n+1}) & \hat{u}_1(\theta_{n+1}) & \hat{u}_2(\theta_{n+1}) & \hat{u}_3(\theta_{n+1}) & \hat{u}_4(\theta_{n+1}) & \hat{u}_5(\theta_{n+1}) \\ \tilde{\zeta}_0(\theta_{n+1}) & \tilde{\zeta}_1(\theta_{n+1}) & \tilde{\zeta}_2(\theta_{n+1}) & \tilde{\zeta}_3(\theta_{n+1}) & \tilde{\zeta}_4(\theta_{n+1}) & \tilde{\zeta}_5(\theta_{n+1}) \\ \tilde{\phi}_0(\theta_{n+1}) & \tilde{\phi}_1(\theta_{n+1}) & \tilde{\phi}_2(\theta_{n+1}) & \tilde{\phi}_3(\theta_{n+1}) & \tilde{\phi}_4(\theta_{n+1}) & \tilde{\phi}_5(\theta_{n+1}) \end{bmatrix}_n . \tag{11b}$$

The real displacement instead of the non-dimensional displacement is used in equation (11a). Therefore, $\hat{U}_0 = L\tilde{U}(\theta_n)$, $\hat{U}_1 = L\tilde{U}(\theta_{n+1})$, $\hat{u}_p(\theta) = L\tilde{u}_p(\theta)$ and $\hat{u}_i(\theta) = L\tilde{u}_i(\theta)$, where $i = 0, 1, 2, \ldots, 5$ in equations (11). The subscript n for the vectors and matrices represents the relations for the nth element. $(\hat{U}_0\ \tilde{Z}_0\ \tilde{\Phi}_0\ \hat{U}_1\ \tilde{Z}_1\ \tilde{\Phi}_1)_n^T$ is the vector of the end displacements for the nth element, whose sign convection is shown in Figure 3. For the nth element, η in equations (7) and (8) is set equal to $(\theta_n + \theta_{n+1})/2$.

From equations (2) and (11a), the end stress resultants for the nth element can be expressed in terms of the end displacements as

$$\begin{Bmatrix} \tilde{Q}_0 \\ \tilde{M}_{z0} \\ \tilde{M}_{t0} \\ \tilde{Q}_1 \\ \tilde{M}_{z1} \\ \tilde{M}_{t1} \end{Bmatrix}_n = [\tilde{k}]_n \begin{Bmatrix} \hat{U}_0 \\ \tilde{Z}_0 \\ \tilde{\phi}_0 \\ \hat{U}_1 \\ \tilde{Z}_1 \\ \tilde{\Phi}_1 \end{Bmatrix}_n + \{\tilde{f}_p\}_n, \tag{12}$$

where

$$[k]_n = (EA)_n([\alpha_1]_n + [\alpha_2]_n)[\beta]_n^{-1}, \tag{13a}$$

$$\{\tilde{f}_p\}_n = -[\tilde{K}]_n \begin{Bmatrix} \hat{u}_p(\theta_n) \\ \tilde{\zeta}_p(\theta_n) \\ \tilde{\phi}_p(\theta_n) \\ \hat{u}_p(\theta_{n+1}) \\ \tilde{\zeta}_p(\theta_{n+1}) \\ \tilde{\phi}_p(\theta_{n+1}) \end{Bmatrix}_n + (EA)_n \begin{Bmatrix} -\lambda_1^2\left[\dfrac{\xi(\theta)_n \hat{u}_p'(\theta_n)}{L} - \tilde{\zeta}_p(\theta_n)\right] \\ \dfrac{\gamma^2}{L\bar{R}(\theta_n)}[\bar{R}(\theta_n)\xi(\theta_n)\zeta_p'(\theta_n) + \tilde{\phi}_p(\theta_n)] \\ -\dfrac{\lambda_2^2\gamma^2}{L\bar{R}(\theta_n)}[\bar{R}(\theta_n)\zeta(\theta_n)\tilde{\phi}_p(\theta_n) - \tilde{\zeta}_p(\theta_n)] \\ \lambda_1^2\left[\dfrac{\xi(\theta_{n+1})\hat{u}_p'(\theta_{n+1})}{L} - \tilde{\zeta}_p(\theta_{n+1})\right] \\ -\dfrac{\gamma^2}{L\bar{R}(\theta_{n+1})}[\bar{R}(\theta_{n+1})\zeta(\theta_{n+1})\tilde{\zeta}_p'(\theta_{n+1}) + \tilde{\phi}_p(\theta_{n+1})] \\ \dfrac{\lambda_2^2\gamma^2}{L\bar{R}(\theta_{n+1})}[\bar{R}(\theta_{n+1})\zeta(\theta_{n+1})\tilde{\phi}_p'(\theta_{n+1}) - \tilde{\zeta}_p(\theta_{n+1})] \end{Bmatrix}, \tag{13b}$$

$$[\alpha_1]_n = [\Lambda_1]_n \begin{bmatrix} \hat{u}_0'(\theta_n) & \hat{u}_1'(\theta_n) & \hat{u}_2'(\theta_n) & \hat{u}_3'(\theta_n) & \hat{u}_4'(\theta_n) & \hat{u}_5'(\theta_n) \\ \tilde{\zeta}_0'(\theta_n) & \tilde{\zeta}_1'(\theta_n) & \tilde{\zeta}_2'(\theta_n) & \tilde{\zeta}_3'(\theta_n) & \tilde{\zeta}_4'(\theta_n) & \tilde{\zeta}_5'(\theta_n) \\ \tilde{\phi}_0'(\theta_n) & \tilde{\phi}_1'(\theta_n) & \tilde{\phi}_2'(\theta_n) & \tilde{\phi}_3'(\theta_n) & \tilde{\phi}_4'(\theta_n) & \tilde{\phi}_5'(\theta_n) \\ \hat{u}_0'(\theta_{n+1}) & \tilde{u}_1'(\theta_{n+1}) & \hat{u}_2'(\theta_{n+1}) & \hat{u}_3'(\theta_{n+1}) & \hat{u}_4'(\theta_{n+1}) & \hat{u}_5'(\theta_{n+1}) \\ \tilde{\zeta}_0'(\theta_{n+1} & \tilde{\zeta}_1'(\theta_{n+1}) & \tilde{\zeta}_2'(\theta_{n+1}) & \tilde{\zeta}_3'(\theta_{n+1}) & \tilde{\zeta}_4'(\theta_{n+1}) & \tilde{\zeta}_5'(\theta_{n+1}) \\ \tilde{\phi}_0'(\theta_{n+1}) & \tilde{\phi}_1'(\theta_{n+1}) & \tilde{\phi}_2'(\theta_{n+1}) & \tilde{\phi}_3'(\theta_{n+1}) & \tilde{\phi}_4'(\theta_{n+1}) & \tilde{\phi}_5'(\theta_{n+1}) \end{bmatrix}_n, \tag{13c}$$

$$[\alpha_2]_n = [\Lambda_2]_n \begin{bmatrix} \tilde{\zeta}_0(\theta_n) & \tilde{\zeta}_1(\theta_n) & \tilde{\zeta}_2(\theta_n) & \tilde{\zeta}_3(\theta_n) & \tilde{\zeta}_4(\theta_n) & \tilde{\zeta}_5(\theta_n) \\ \tilde{\phi}_0(\theta_n) & \tilde{\phi}_1(\theta_n) & \tilde{\phi}_2(\theta_n) & \tilde{\phi}_3(\theta_n) & \tilde{\phi}_4(\theta_n) & \tilde{\phi}_5(\theta_n) \\ \tilde{\zeta}_0(\theta_n) & \tilde{\zeta}_1(\theta_n) & \tilde{\zeta}_2(\theta_n) & \tilde{\zeta}_3(\theta_n) & \tilde{\zeta}_4(\theta_n) & \tilde{\zeta}_5(\theta_n) \\ \tilde{\zeta}_0(\theta_{n+1}) & \tilde{\zeta}_1(\theta_{n+1}) & \tilde{\zeta}_2(\theta_{n+1}) & \tilde{\zeta}_3(\theta_{n+1}) & \tilde{\zeta}_4(\theta_{n+1}) & \tilde{\zeta}_5(\theta_{n+1}) \\ \tilde{\phi}_0(\theta_{n+1}) & \tilde{\phi}_1(\theta_{n+1}) & \tilde{\phi}_2(\theta_{n+1}) & \tilde{\phi}_3(\theta_{n+1}) & \tilde{\phi}_4(\theta_{n+1}) & \tilde{\phi}_5(\theta_{n+1}) \\ \tilde{\zeta}_0(\theta_{n+1}) & \tilde{\zeta}_1(\theta_{n+1}) & \tilde{\zeta}_2(\theta_{n+1}) & \tilde{\zeta}_3(\theta_{n+1}) & \tilde{\zeta}_4(\theta_{n+1}) & \tilde{\zeta}_5(\theta_{n+1}) \end{bmatrix}_n, \tag{13d}$$

and $[\Lambda_i]_n$ $(i = 1, 2)$ are diagonal matrices. The diagonal vector of $[\Lambda_1]_n$ is $\{-\lambda_1^2/\xi(\theta_n), \bar{\gamma}^2 L\xi(\theta_n), -\lambda_2^2\bar{\gamma}^2 L\xi(\theta_n), \lambda_1^2\xi(\theta_{n+1}), -\bar{\gamma}^2 L\xi(\theta_{n+1}), \lambda_2^2\bar{\gamma}^2 L\xi(\theta_{n+1})\}$ while the diagonal vector of $[\Lambda_2]_n$ is $\{\lambda_1^2 L, \bar{\gamma}^2 L^2/R(\theta_n), \lambda_2^2\bar{\gamma}^2 L^2/R(\theta_n), -\lambda_1^2 L, -\bar{\gamma}^2 L^2/R(\theta_{n+1}), -\lambda_2^2\bar{\gamma}^2 L^2/R(\theta_{n+1})\}$. $[\tilde{k}]_n$ is the so-called local dynamic stiffness matrix of the nth element, and $\{\tilde{f}_p\}_n$ is the equivalent nodal external loading for the nth element. The sign convention for the nodal stress resultants is also shown in Figure 3.

Using the continuity conditions between adjacent elements, namely, the continuity in the displacement, rotation, and stress resultants, the global dynamic stiffness matrix, $[\tilde{K}]$, of the system can be obtained by superposing the local dynamic stiffness matrices of all the elements. Consequently, one can obtain the following relations:

$$[\tilde{K}]\{\tilde{\mathbf{U}}\} = \{\tilde{\mathbf{F}}\}, \tag{14}$$

where $\{\tilde{U}\}$ is the end displacement vector for the curved beam system under consideration while $\{F\}$ is the equivalent external loading vector applied at the ends of each element.

By substituting boundary conditions into equation (14), one can solve precisely the unknown end displacement vector from equation (14) using any conventional linear solver. Then, in the Laplace domain, the displacement components and stress resultants at any desired locations can be computed after the series solution for each element is determined from equations (10) and (11).

To analyze the free vibration of curved beams with variable curvature, one can leave off the damping forces and external loading in equations (6) and replace the Laplace transform parameter s with $i\omega$. Consequently, equation (14) can be reduced to

$$\begin{bmatrix} [\tilde{K}_{uu}] & [\tilde{K}_{ub}] \\ [\tilde{K}_{bu}] & [\tilde{K}_{bb}] \end{bmatrix} \begin{Bmatrix} \{\tilde{\mathbf{U}}_u\} \\ \{\tilde{\mathbf{U}}_b\} \end{Bmatrix} = \begin{Bmatrix} \{\mathbf{0}\} \\ \{\tilde{\mathbf{F}}_b\} \end{Bmatrix}, \tag{15}$$

where $\{\tilde{\mathbf{U}}_u\}$ is the vector corresponding to the unknown end vibratory displacement components, $\{\tilde{\mathbf{U}}_b\}$ is the vector of the prescribed vibratory displacement components on the boundaries, and $\{\tilde{\mathbf{F}}_b\}$ is the vector of unknown vibratory stress resultants on the

displacement prescribed boundaries. In free vibration problems, $\{\tilde{U}_b\}$ is usually a zero vector. Then, equation (15) reduces to

$$[\tilde{K}_{uu}]\{\tilde{\mathbf{U}}_u\} = \{0\}, \tag{16}$$

from which one can find the eigenvalues and the corresponding eigenvectors. The natural frequencies are the value of ω resulting in the determinant of $[\tilde{K}_{uu}]$ equal to zero.

5. NUMERICAL LAPLACE INVERSION

After obtaining exactly the responses of the displacement components and stress resultants at the locations of interest in the Laplace domain, these results have to be transformed back into the time domain to complete the analysis. The algorithm developed by Durbin [25] is adopted to find the inverse Laplace transforms.

The inverse of the Laplace transform of a function is defined as

$$f(t) = \frac{1}{2\pi i}\int_{\bar{a}-\mathrm{i}\infty}^{\bar{a}+\mathrm{i}\infty} \mathrm{e}^{st}\tilde{f}(s)\,\mathrm{d}s, \tag{17}$$

where $\bar{a} > 0$ is arbitrary but is greater than the real parts of all the singularities of $\tilde{f}(s)$. Following Durbin's technique,

$$f(t_j) \approx (2\,\mathrm{e}^{\mathrm{i}\bar{a}\Delta t}/t_{max})\left\{-(1/2)\,\mathrm{Re}\,[\tilde{f}(\bar{a})] + \mathrm{Re}\left[\sum_{n=0}^{N_t-1}(F(n)+\mathrm{i}G(n))W^{jn}\right]\right\}, \tag{18}$$

where

$$F(n) = \sum_{m=0}^{M}\mathrm{Re}\,[\tilde{f}(\bar{a}+\mathrm{i}(n+mN_t)2\pi/t_{max})], \qquad G(n) = \sum_{m=0}^{M}\mathrm{Im}\,[\tilde{f}(\bar{a}+\mathrm{i}(n+mN_t)2\pi/t_{max})],$$

and $W = \mathrm{e}^{\mathrm{i}2\pi/N_t}$, t_{max} is the time interval of interest for the problem under consideration, and $\Delta t = t_{max}/N_t$. The computations involved in equation (18) can be accelerated by employing the fast Fourier transform algorithm. The accuracy of Durbin's algorithm is generally dependent on the values of MN_t (the product of M and N_t), t_{max} and $\bar{a}$. Generally speaking, the numerical error decreases for increasing values of $\bar{a}t_{max}$ and MN_t. The typical values for these parameters, as suggested by Durbin, are $MN_t = 50$ to 5000 and $\bar{a}t_{max} = 5$ to 10.

6. NUMERICAL EXAMPLES

As numerical examples, the responses of two-span continuous elliptic beams with $a/b = 2$, 3, and 4 subjected to a rectangular impulse at $\theta = 67{\cdot}5^\circ$ (see Figure 4) will be investigated. In the following, the characteristic length of the curved beam in the formulation, L, is set equal to $2a$. The impulse is defined as

$$P_p(t) = EA\bar{\gamma}[U(t-0{\cdot}1) - U(t-0{\cdot}12)], \tag{19}$$

where $U(t)$ is a unit step function. Hence, the rectangular impulse starts from $t = 0{\cdot}1$ s and ends at $t = 0{\cdot}12$ s. The boundary conditions are prescribed as $u = \phi = M_z = 0$ at $\theta = 0^\circ$ (hinged support), $u = 0$ at $\theta = 45^\circ$ and $u = M_t = M_z = 0$ at $\theta = 90^\circ$ (roller support). The

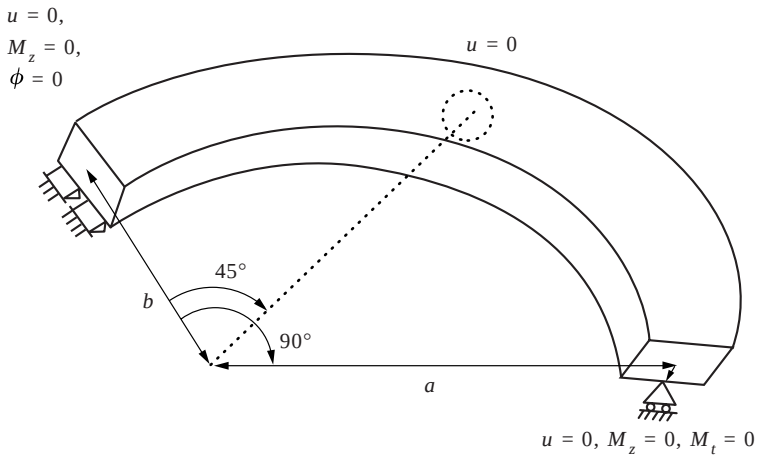

Figure 4. A sketch of a two-span elliptic beam.

properties of the curved beams with square cross-sections are specified as: $\sqrt{E/\rho} = 5000$ m/s, Poisson ratio $(v) = 0{\cdot}3$, $a = 30$ m, and $1/\bar{\gamma} = 70$. Furthermore, the damping effects are neglected.

Table 1 lists the first five natural frequencies for the elliptic beams under consideration, which were obtained by decomposing the curved beam into 12 elements and using 15 geometric terms and 20 solution terms for each element. The details of the free vibration analysis have been given by Huang *et al*. [14]. It is believed that the listed results are convergent to at least five significant figures. The results show that the frequency decreases with a decrease of a/b for each mode.

Figures 5 and 6 show the responses for the case where $a/b = 3$, in which the responses are expressed in terms of the non-dimensional quantities defined as $\bar{u} = u/L$, $Q^* = Q/(\kappa GA)$, $M_z^* = M_z L/(EI)$, and $M_t^* = M_t L/C$. Careful examination of the responses of non-dimensional shear forces at $\theta = 67{\cdot}499^\circ$ and $67{\cdot}501^\circ$, as shown in Figure 5, reveals that the sum of these responses in terms of the real shear forces almost exactly matches the input rectangular impulse at $\theta = 67{\cdot}5^\circ$. This coincidence somewhat demonstrates the accuracy of the results obtained using the proposed procedure. Investigation of the responses at the load point ($\theta = 67{\cdot}5^\circ$), as shown in Figure 6, reveals that the responses of the stress resultants have higher frequency components than do those

TABLE 1

Natural frequencies (rad/s) for two-span elliptic beams

	a/b		
Mode	2	3	4
1	88·3783	96·2593	100·603
2	150·895	164·910	166·772
3	259·200	303·416	325·097
4	350·180	371·402	385·364
5	409·024	474·661	505·543

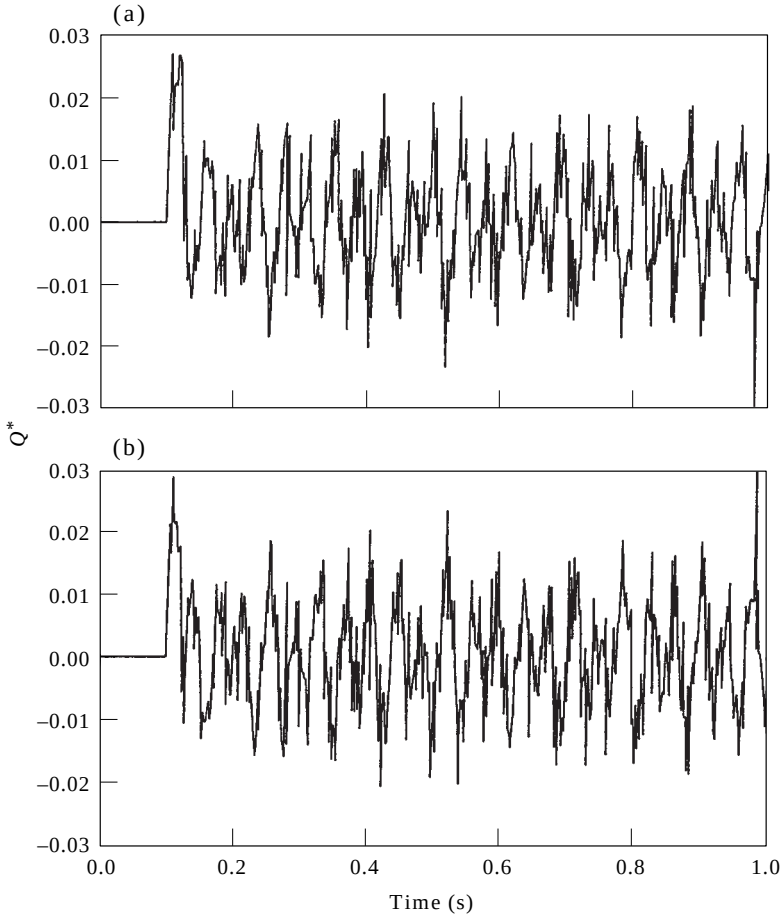

Figure 5. Variation of Q^*: (a) at $\theta = 67{\cdot}499^\circ$ and (b) $\theta = 67{\cdot}501^\circ$.

for the displacement components as expected. The results in these figures show no Gibb's phenomenon.

Figure 7 shows the maximum dynamic non-dimensional responses along the two-span curved beam normalized by the maximum static non-dimensional responses caused by a static loading at $\theta = 67{\cdot}5^\circ$ with the same amplitude as the impulse. The results somewhat show the dynamic effects of the impulse on the responses of the elliptic beam with different ratios of a/b. When a/b varies from 2 to 4, the maximum values of $\bar{u}_{d,max}/\bar{u}_{s,max}$, $\zeta_{d,max}/\zeta_{s,max}$, and $\phi_{d,max}/\phi_{s,max}$, respectively, occur around $\theta = 20^\circ$, 90° and 75°, while the maximum values of $Q^*_{d,max}/Q^*_{s,max}$ and $M^*_{zd,max}/M^*_{zs,max}$ occur at the middle support. The maximum value of $M^*_{td,max}/M^*_{ts,max}$ occurs at the left-hand support for $a/b = 3$ and 4 while it occurs around $\theta = 53^\circ$ for $a/b = 2$. Careful investigation of the responses of $Q^*_{d,max}/Q^*_{s,max}$ reveals that a jump occurs at $\theta = 45^\circ$, which results from the reaction force at the middle support. The dynamic effects of the impulse on the responses of the curved beams obviously depend on the geometry of the curved beam and the location of the response as well as on the physical quantity of the response to be considered. As a matter of fact, the effects of impulse are also dependent on the duration and the position of the applied impulse, which were given in Chang's thesis [26].

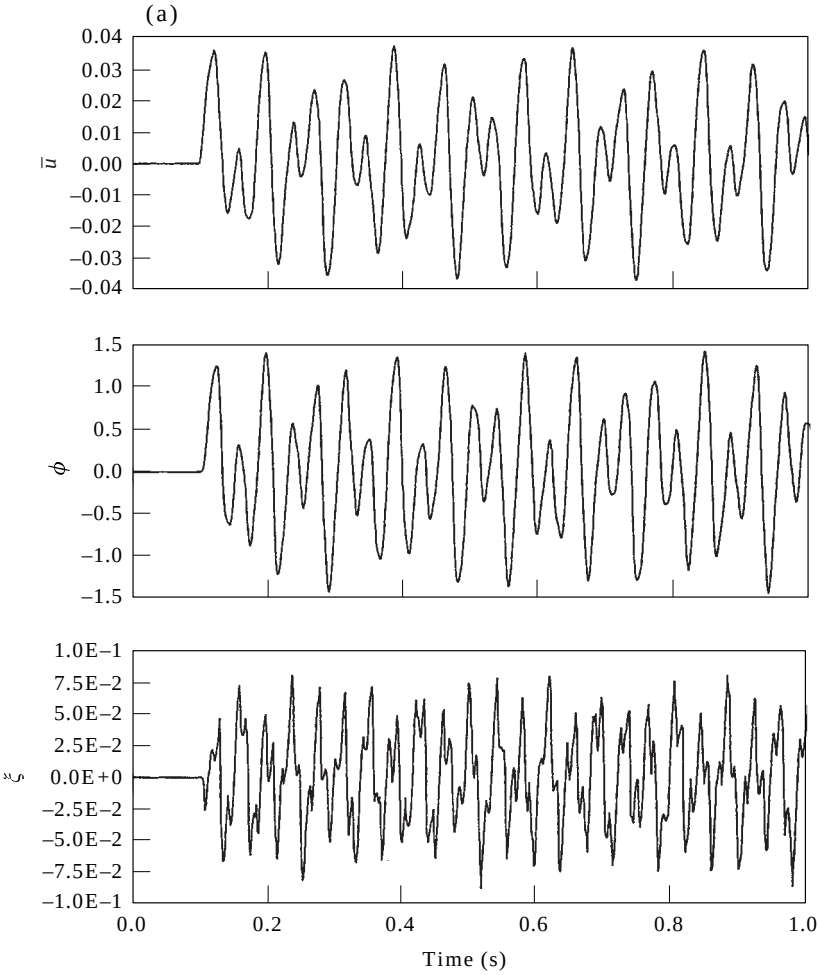

Figure 6(a)—(*Caption on next page*).

7. CONCLUDING REMARKS

This paper has presented a systematic procedure for analyzing the out-of-plane dynamic behaviours of curved beams with variable curvature. The solution has been developed by combining the Laplace transformation with the dynamic stiffness method, in which the first known transformed dynamic stiffness matrix and the equivalent nodal loading vector for non-circular curve beams subjected to distributed loading are formulated based on a series solution obtained using the Frobenius method. Since an analytical solution in the Laplace domain is used to compute the stress resultants at any location of interest, the obtained responses of the stress resultants in the time domain are highly accurate, which is not easy to accomplish using other methods. The free vibration analysis can be performed by means of a simple modification in the formulation presented, which results in an exact soution.

Application of the proposed solution to transient analysis has been carried out to investigate the dynamic behaviours of two-span elliptic curved beams with $a/b = 2,\ 3$

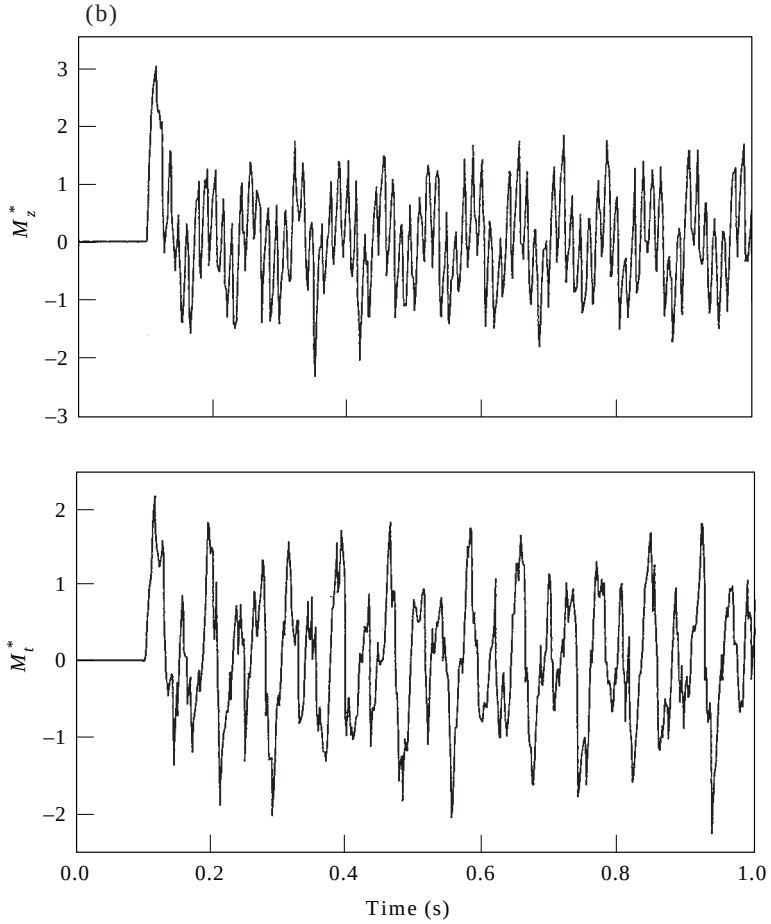

Figure 6. (a) Variation of the displacement components at $\theta = 67{\cdot}5^\circ$. (b) Variation of M_z^* and M_t^* at $\theta = 67{\cdot}5^\circ$.

and 4, subjected to a rectangular impulse at the middle of the second span. The time responses of the displacement components and stress resultants at the load point have been shown to demonstrate the high degree of accuracy of the proposed solution. Generally speaking, the maximum values for the ratios of the maximum dynamic responses to the maximum static responses vary from 1·5 to 3·0, depending on the physical quantities under consideration and a/b. Furthermore, the ratios also significantly depend on the duration of the impulse, the locations of the applied impulse and the responses considered.

The proposed solution can be applied to solve more complicated problems, such as the transient responses of frameworks and arch bridges composed of curved elements, by combining it with the dynamic stiffness matrices of other types of elements. Furthermore, based on the correspondence principle, the present solution is also suitable for viscoelasticity problems, which become more common when viscoelastic materials are used in passive control systems to reduce the dynamic responses of structures. Finally, with a simple modification, the solution given in the paper can be applied in a straightforward manner to analysis of the stochastic responses of curved beams [27].

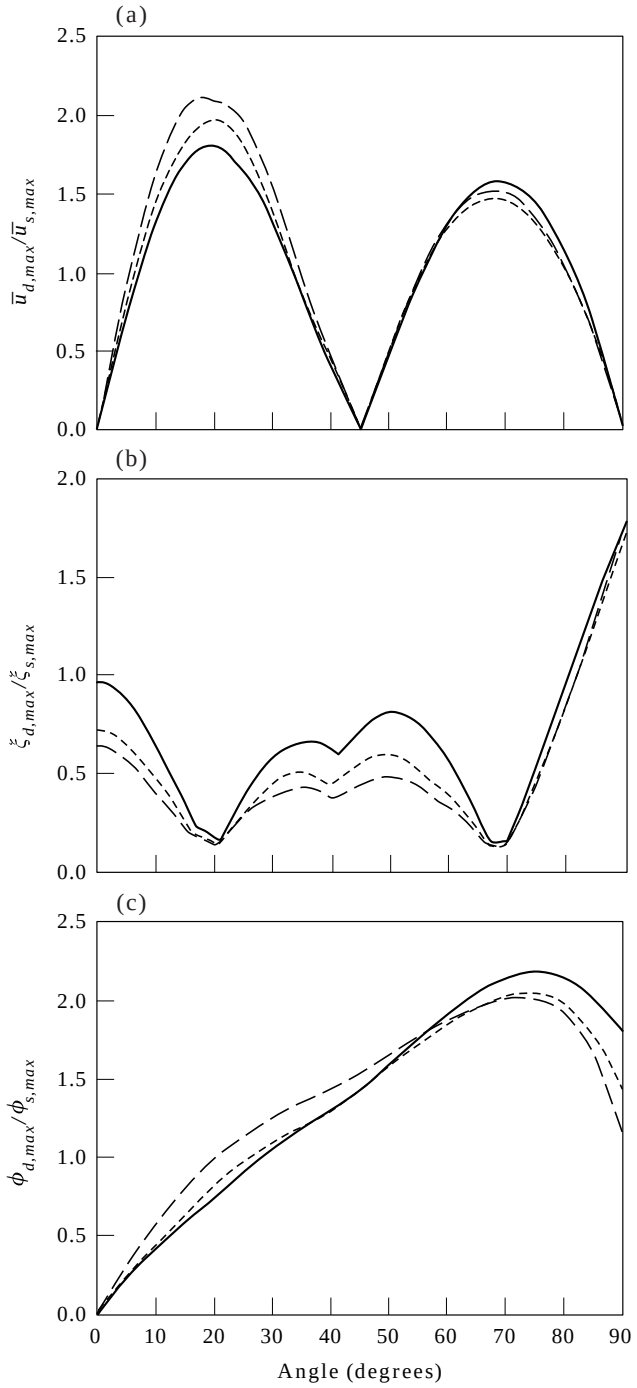

Figure 7(a–c)—(*Caption on next page*).

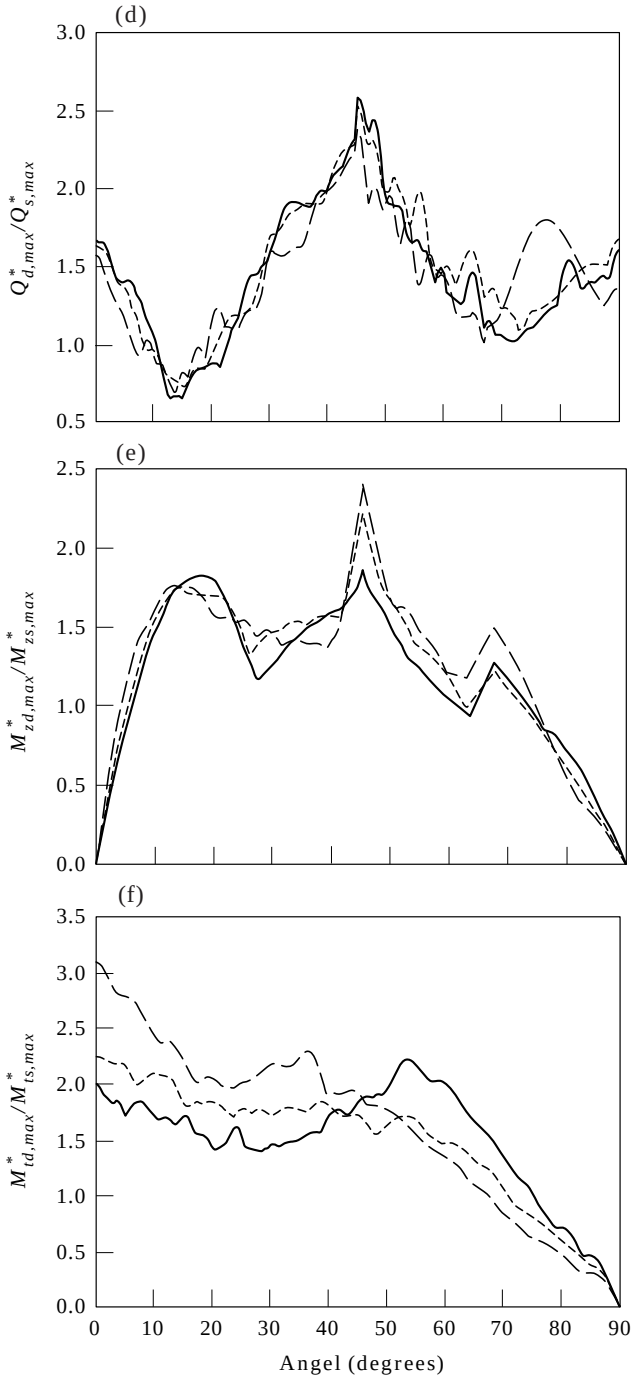

Figure 7(d–f).

Figure 7. The ratios of the maximum dynamic responses to the maximum static responses. ——, $a/b=2$; ---, $a/b=3$; —·—, $a/b=4$.

ACKNOWLEDGMENTS

This research was supported by the National Science Council, R.O.C. (NSC 87-2211-E-032-015), which is gratefully acknowledged. Appreciation is also extended to colleagues at the National Center for Research on Earthquake Engineering for their kind support in finishing this work.

REFERENCES

1. P. F. McManus and G. A. Nasir 1969 *Journal of the Structure Division, Proceedings of the American Society of Civil Engineers* 95, 853–870. Horizontally curved girders—state of the art.
2. S. Markus and T. Nanasi 1981 *The Shock and Vibration Digest* **13**, 3–14. Vibration of curved beams.
3. P. A. A. Laura and M. J. Maurizi 1987 *The Shock and Vibration Digest* **19**, 6–9. Recent research on vibrations of arch-type structures.
4. P. Chidamparam and A. W. Leissa 1993 *Applied Mechanics Reviews* **46**, 467–483. Vibrations of planar curved beams, rings, and arches.
5. E. Volterra and J. D. Morell 1961 *Journal of Applied Mechanics* **28**, 624–627. Lowest natural frequency of elastic arc for vibrations outside the plane of initial curvature.
6. T. M. Wang 1975 *Journal of Sound and Vibration* **42**, 515–519. Fundamental frequency of clamped elliptic arcs for vibrations the plane of initial curvature.
7. T. C. Chang and E. Volterra 1969 *The Journal of the Acoustical Society of America* **46**, 1165–1174. Upper and lower bounds for frequencies of elastic arcs.
8. T. C. Chang and E. Volterra 1970 *The Journal of the Acoustical Society of America* **49**, 370–371. Natural frequencies of simply supported arcs.
9. M. Kawakami, T. Sakiyama, H. Matsuda and C. Morita 1995 *Journal of Sound and Vibration* **187**, 381–401. In-plane and out-of-plane free vibrations of curved beams with variable sections.
10. S. Takahashi and K. Suzuki 1977 *Bulletin of the Japanese Society of Mechanical Engineers* **20**, 1409–1416. Vibrations of elliptic arc bar perpendicular to its plane.
11. K. Suzuki, H. Aida and I. Takahashi 1978 *Bulletin of the Japanese Society of Mechanical Engineers* **21**, 1685–1695. Vibrations of curved bars perpendicular to their planes.
12. K. Suzuki and S. Takahashi 1981 *Bulletin of the Japanese Society of Mechanical Engineers* **24**, 1206–1213. Out-of-plane vibrations of curved bars considering shear deformation and rotary inertia.
13. T. Irie, G. Yamada and I. Takashashi 1982 *Journal of the Applied Mechanics* **49**, 439–441. Free out-of-plane vibration of arcs.
14. C. S. Huang, Y. P. Tseng and S. H. Chang 1997 *Chinese Journal of Mechanics* **14**, 349–361. An analytical solution for out-of-plane vibration of an arch.
15. T. Irie, G. Yamada and I. Takashashi 1986 *Journal of Sound and Vibration* **71**, 145-156. The steady state out-of-plane response of a Timoshenko curved beam with internal damping.
16. K. Suzuki, K. Sugi, T. Kosawada and S. Takahashi 1986 *Bulleting of the Japanese Society of Mechanical Engineers* **29**, 4312–4317. Out-of-plane impulse response of a curved bar with varying cross-section.
17. C. S. Huang, Y. P. Tseng and C. R. Lin 1997 *Journal of Engineering Mechanics, Proceedings of the American Society of Civil Engineers* (accepted). In-plane transient responses of an arch with variable curvature using the dynamic stiffness method with numerical Laplace transform.
18. G. D. Manolis and D. E. Beskos 1982 *Computer and Structures* **15**, 521–531. Dynamic response of framed underground structures.
19. G. V. Narayanan and D. E. Beskos 1982 *Engineering Structure* **4**, 53–62. Dynamic soil–structure interaction by numerical Laplace transform.
20. D. E. Beskos and G. V. Narayanan 1983 *Computer Method in Applied Mechanics and Engineering* **37**, 289–307. Dynamic response of frameworks by numerical Laplace transform.
21. E. T. Whittaker and G. N. Watson 1965 *A Course of Modern Analysis*. Cambridge: Cambridge University Press; fourth edition.
22. R. L. Mindlin and L. E. Goodman 1950 *Journal of Applied Mechanics* **17**, 373–380. Beam vibrations with time dependent boundary conditions.
23. G. R. Cowper 1966 *Journal of Applied Mechanics* **33**, 335–340. The shear coefficients in Timoshenko's beam theory.

24. S. P. TIMOSHENKO and J. N. GOODIER 1970 *Theory of Elasticity*. New York: McGraw-Hill; third edition.
25. F. DURBIN 1974 *Computer Journal* **17**, 371–376. Numerical inversion of Laplace transforms: an efficient improvement to Dubner and Abate's method.
26. S. H. CHANG 1997 *M.S. thesis*, *Tamkang University*, *Taiwan*. Out-of-plane dynamic analysis for arches of variable cross-section and variable curvature.
27. C. S. HUANG, Y. P. TSENG and C. R. LIN 1997 *Mechanics of Structures and Machines* (submitted). An accurate solution for the in-plane stochastic responses of arches with variable curvature subjected to base excitation.